ELSEVIER

Polymer 41 (2000) 7511–7522

polymer

Effect of epoxidation on the transport behaviour and mechanical properties of natural rubber

T. Johnson, S. Thomas*

School of Chemical Sciences, Mahatma Gandhi University, Priyadarshini Hills P.O., Kottayam 686 560, Kerala, India

Received 24 November 1997; received in revised form 15 June 1998; accepted 21 January 2000

Abstract

Several modifications of natural rubber (NR) have been tried by various researchers and are extensively reported in the literature. Among these modifications, epoxidation has special significance, as it combines several important properties such as oil resistance, low air permeability, strain crystallising nature and improved damping. The effect of epoxidation on the transport characteristics and mechanical behaviour of NR has been studied in this work. Epoxidised natural rubber (ENR) with 25 and 50 mol% epoxidation level (ENR-25 and ENR-50) has been used besides NR. Different transport parameters such as rate constant, diffusion and permeation coefficients and sorption coefficient have been computed. From the temperature dependence of diffusion, activation parameters were evaluated. A comparison between theoretical and experimental diffusion results was carried out to understand the mechanism of diffusion. The polymer network structure in the swollen state has been analysed by applying the affine and phantom models. Mechanical properties of unswollen, swollen and deswollen samples were specially investigated.

Keywords: Epoxidised natural rubber; Diffusion; Molecular transport

1. Introduction

The use of polymers as structural engineering materials [1–3] is increasing in recent years. This makes it important to study the effect of external forces such as presence of solvents, temperature etc. on polymer properties. Most polymer products show a reduction in polymer property due to swelling and relaxation of chain segments when brought into contact with organic chemicals. Therefore the important requirement of a membrane material for commercial application is that it should be chemically resistant and should retain its mechanical strength and dimensional stability. This suggests that the basic transport phenomenon play a prominent role in many industrial and engineering applications [4–9].

Many researchers have been using the gravimetric method as a rapid and convenient means of studying polymer–solvent interactions. Transport behaviour of polyurethane in a series of aliphatic alcohols was studied by Hung and Autian [10] using the gravimetric method. Sefton and Mann [11] studied the rate of absorption of benzene by open cell polyurethane foam. Schneider et al. [12] investigated the sorption and diffusion of a series of liquids through polyurethane membrane and analysed how this behaviour was influenced by the choice of solvent and the heterophase nature of polymer. Chiang and Sefton [13] used diffusion analysis to investigate the morphology of styrene–butadiene–styrene (SBS) triblock copolymer. Swelling behaviour and mechanical properties of end linked poly(dimethyl siloxane) networks and randomly crosslinked polyisoprene networks have been studied by Rennar and Oppermann [14]. Jain et al. [15] studied the swelling characteristics and mechanical properties of copolyurethanes cured with trimethyl propane and triethanol amine. Recently in this laboratory, transport properties of various elastomeric membranes were investigated by gravimetric method [16–19]. The experimental results have been compared with theoretical predictions.

In this paper, we have studied the effect of epoxidation on the mechanical and transport properties of natural rubber (NR) which is an industrially important polymer. Epoxidised natural rubber (ENR) combines the oil resistance of acrylonitrile–butadiene rubber (NBR), low air permeability of butyl rubber [20,21] and strain crystallising nature of NR [22]. Mechanical properties of unswollen, swollen and deswollen samples were specially studied.

* Corresponding author. Tel.: + 91-81-598015; fax: + 91-481-561190.
E-mail address: sabut@md4.vsnl.net.in (S. Thomas).

0032-3861/00/$ - see front matter
PII: S0032-3861(00)00076-8

Table 1
Compounding recipe (Parts per hundred parts of rubber by weight)

Ingredients	NR	ENR-25	ENR-50
ZnO	5	5	5
Stearic acid	2	2	2
Calcium stearate	0	3	3
CBS[a]	1.5	1.5	1.5
Sulphur	2.5	1.5	1.5
TDQ[b]	1	1	1

[a] *N*-Cyclohexyl-2-benzothiazyl sulphenamide.
[b] Trimethyl di-hydro quinoline.

2. Experimental

Indian standard natural rubber (ISNR-5) was supplied by RRII, Kottayam, India. Epoxidised natural rubber–epoxyprene with 25 mol% epoxidation (ENR-25) and epoxyprene with 50 mol% epoxidation (ENR-50) were supplied by Rubber Research Institute, Malaysia. The number average molecular weight ($\bar{M}_n$) of all the three rubber is in the range of 1×10^6–9.9×10^5. Compounding was carried out on a two-roll mixing mill (friction ratio 1:1.4), according to ASTM D15-627. The basic formulation used is given in Table 1. The compounds were then compression moulded along the mill grain direction using an electrically heated hydraulic press at 150°C.

2.1. Swelling experiment

Circular samples of diameter 1.9 cm were used for sorption experiments. Thickness of the samples was measured using a micrometer. Samples were immersed in solvents taken in test bottles and kept at constant temperature in an air oven. The samples were weighed at periodic intervals. The weighing were continued till equilibrium swelling is attained. The weighing was accurate up to 0.001 g. The SEM observations of surface morphology of NR, ENR-25 and ENR-50 were made using a JEOL-JSM-35C model scanning electron microscope.

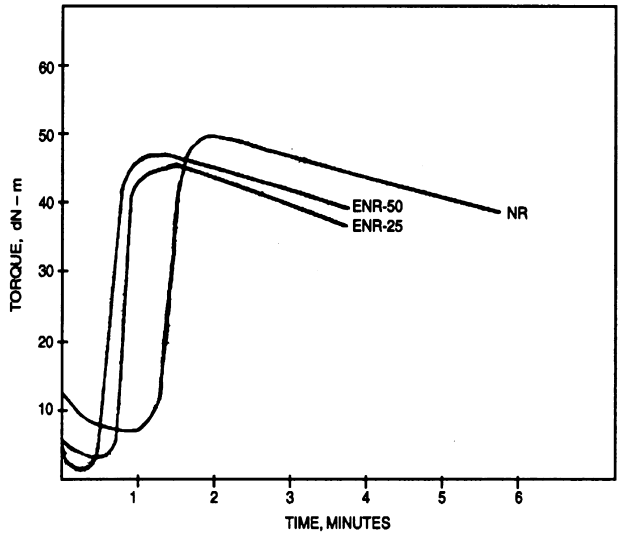

Fig. 1. Rheograph of NR, ENR-25 and ENR-50.

2.2. Physico-mechanical testings

The experiments were carried out using a universal testing machine (UTM) at 27°C with a crosshead speed of 500 mm/min. using dumbbell shaped tensile specimens according to ASTM D412-80. The testings were carried out with swollen, unswollen and deswollen samples.

3. Results and discussion

3.1. Processing characteristics

Rheographs of NR, ENR-25 and ENR-50 compounds are given in Fig. 1. The processing characteristics are presented in Table 2. Usually the minimum torque or viscosity (M_L) is a measure of the filler contents in the system. Since these are unfilled compounds, M_L is a measure of the extent of mastication. The M_L values decrease from NR to ENR-50. This may be due to the extensive mastication and resulting chain scission in ENR. The maximum torque or viscosity (M_H) is a direct measure of the crosslink density in the sample. Since M_H decreases from NR to ENR-50, the crosslink density is expected to decrease. The trend of optimum torque is also similar. The variation of optimum cure time (t_{90}), rheometric scorch time (t_2) and rheometric induction time (t_1) are also presented in Table 2. With increasing epoxy content, these values register a decrease. This may be due to the presence of unreacted calcium stearate added to counteract acid release in ENR during compounding. Calculating the cure rate index (CRI) as given below can roughly assess the fastness of the curing reaction

$$\mathrm{CRI} = \frac{100}{t_{90} - t_2}\,\mathrm{time}^{-1} \tag{1}$$

and more systematically by the rate constant values. Assuming the cure reaction to be first order, the rate constants can be calculated from the cure curves [23]. CRI values first increase from NR to ENR-25 and then decrease for ENR-50. The increase for ENR-25 may be due to the presence of

Table 2
Cure characteristics

Properties	NR	ENR-25	ENR-50
M_L (dN m)	7	3.5	1.5
M_H (dN m)	50	45.5	47
Optimum cure torque (dN m)	45.7	41.3	40.9
t_{90} (ms)	8.25	4.75	4.00
t_2 (ms)	6.00	3.75	2.50
t_1 (ms)	5.5	3.25	2.25
CRI (min^{-1})	44.44	100	66.66
k (min^{-1})	0.885	1.392	1.340

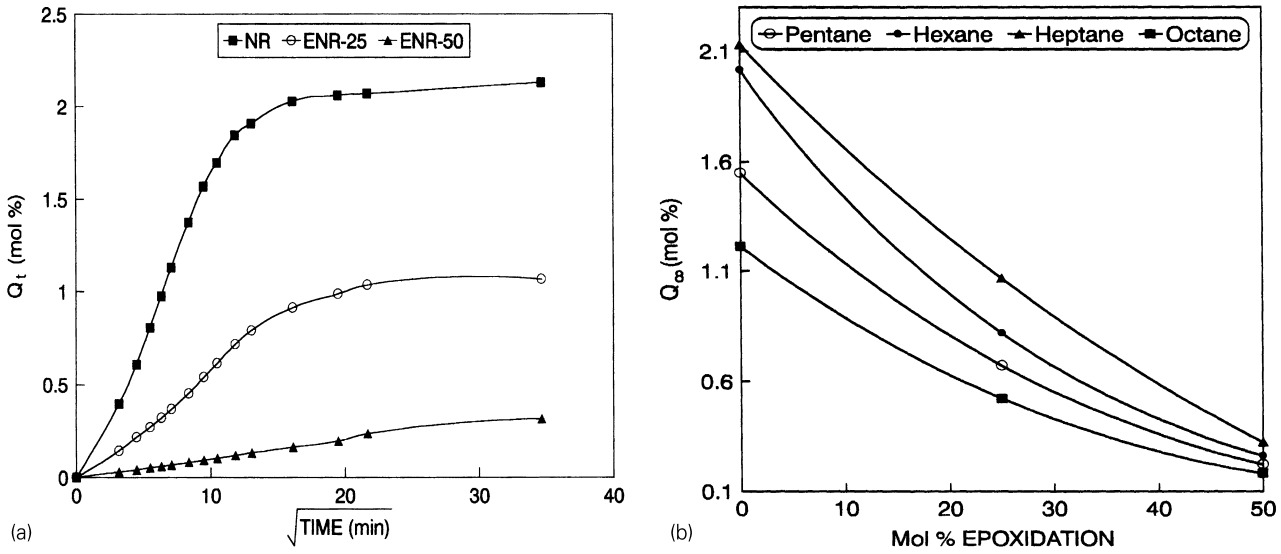

Fig. 2. (a) Q_t mole percent uptake of hexane by NR, ENR-25 and ENR-50. (b) Variation of maximum mole percent uptake with epoxidation.

more unreacted calcium stearate compared to ENR-50. The *k* values also follow the same order.

3.2. Effect of epoxidation

The effect of epoxidation on solvent uptake is clearly manifested in Fig. 2a and b. The figures indicate that NR has the maximum uptake whereas ENR-50 the lowest. This may be explained by the inherent solvent resistance [24] of ENR. The structure of NR and ENR is given in Fig. 3. The epoxy group reduces the chain flexibility with a consequent increase in T_g values (NR = −72°C, ENR-25 = −47°C, ENR-50 = −27°C). Also the polar nature of ENR chain increases the interchain interaction and this factor also contributes to the decreased chain flexibility. The unswollen and swollen state of NR and ENR indicates that the epoxy groups decrease the solvent uptake in ENR.

The mole percent uptake of solvents in ENR-25 with increasing penetrant size is shown in Fig. 4. This figure indicates that Q_∞ values increase from pentane to heptane. However, octane shows the lowest uptake. This observation can be explained on the basis of the solubility parameter difference between the polymer and penetrant. The difference in the solubility parameters between the polymer and the penetrant is often used to characterise the sorption behaviour of the penetrant in the polymer membrane [25,26]. The solubility of the penetrant generally becomes high when the difference in the solubility parameters between the polymer and the penetrant is small. The solubility parameter difference for different polymer–solvent systems is given in Table 3. Though this value is lowest for octane, the lowest uptake for octane is due to its larger size compared to pentane, hexane and heptane. For the other three solvents, the uptake is in accordance with the solubility parameter difference.

Figs. 5–7 show the effect of temperature and epoxidation level on mole per cent uptake of hexane. The rate of diffusion increases with temperature, but the maximum solvent uptake decreases for NR whereas it increases for ENR-25 and ENR-50 with increase in temperature. This increase in

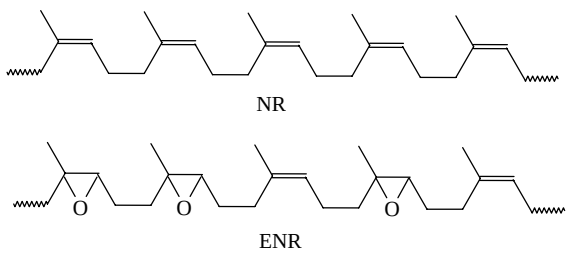

Fig. 3. Structure of NR and ENR.

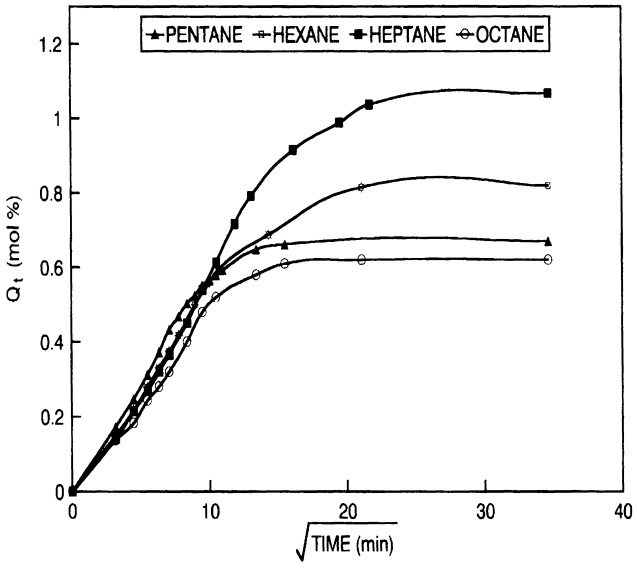

Fig. 4. Mole percent uptake of ENR-25 in different solvents at 27°C.

Table 3
Solubility parameter difference (kJ/mol)

Solvent	NR	ENR-25	ENR-50
Pentane	1.9	3.1	3.9
Hexane	1.5	2.7	3.5
Heptane	1.1	2.3	3.1
Octane	0.7	1.9	2.7

solvent uptake can be attributed to the presence of a highly crosslinked gel phase in ENR. Epoxidation results in a highly crosslinked gel phase and a lightly crosslinked sol phase [27,28]. This results in a two-phase morphology for ENR. The gel phase has been estimated according to ASTM D3616 and the value for ENR-25 is around 47% and for ENR-50 around 75%. Surface morphology of NR, ENR-25 and ENR-50 given in Fig. 8 shows the highly crosslinked gel phase in ENR. The SEM photograph of NR shows a smooth surface morphology. This reveals the presence of a uniform crosslink density throughout the matrix. In ENR-25, a two-phase morphology is observed. The increased gel content in ENR-50 results in a well-defined two-phase morphology compared to ENR-25. The highly crosslinked gel phase makes the ENR matrix more compact and the chain flexibility is reduced compared to NR. However, with increase in temperature, the chain flexibility increases which increase the maximum mole percent uptake in ENR with temperature. This is further explained by the enthalpy of sorption discussed in a later section.

3.3. Sorption, desorption, resorption and redesorption (S–D–RS–RD)

By the usual method, sorption process was carried out in polymer samples. After complete sorption, the sorbed samples were placed in a vacuum oven at constant temperature for desorption measurements. The desorbed samples were again exposed to solvents for resorption followed by redesorption. Sorption, desorption, resorption and redesorption curves for NR, ENR-25 and ENR-50 are shown in Figs. 9–11. It is clear from the figures that, a mass loss is observed in NR during sorption–desorption cycle. Q_∞ mole percent value for desorption cycle is higher suggesting a mass loss during desorption. While for ENR-25 and ENR-50 the Q_∞ values decrease indicating a mass gain. The mass loss in NR may be due to leaching out of the unreacted compounding ingredients whereas in the case of ENR, the solvent

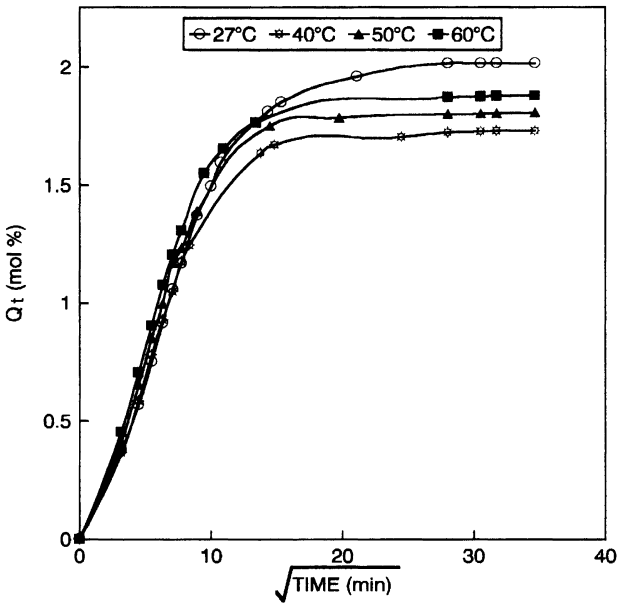

Fig. 6. Effect of temperature on mole percent uptake of hexane in ENR-25.

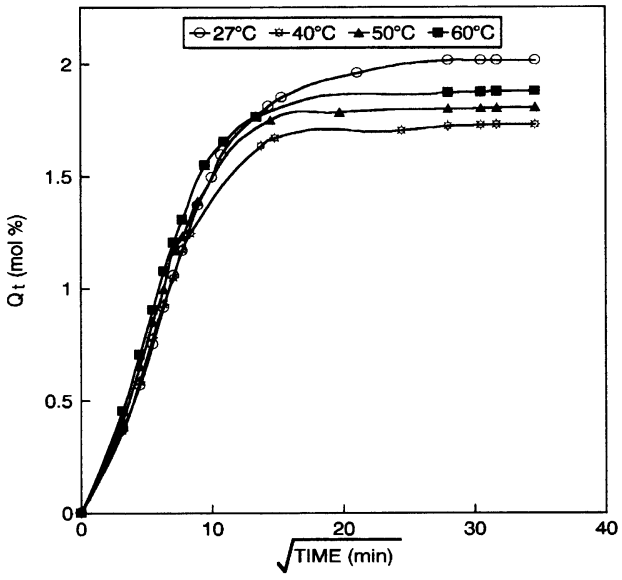

Fig. 5. Effect of temperature on mole percent uptake of hexane in NR.

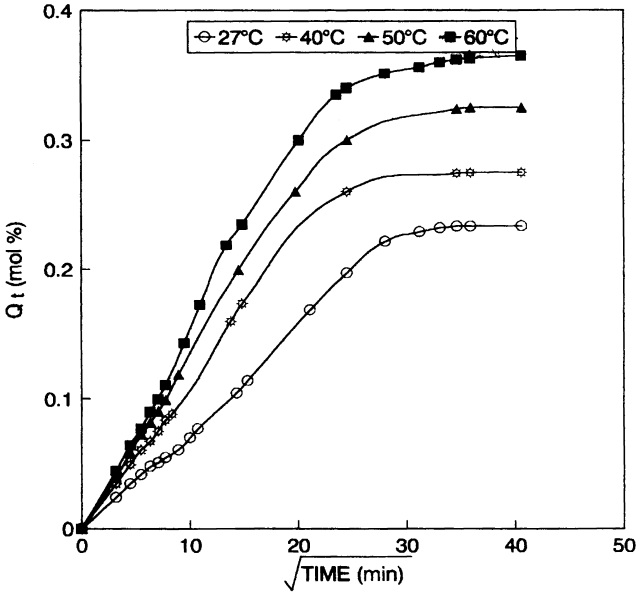

Fig. 7. Effect of temperature on mole percent uptake of hexane in ENR-50.

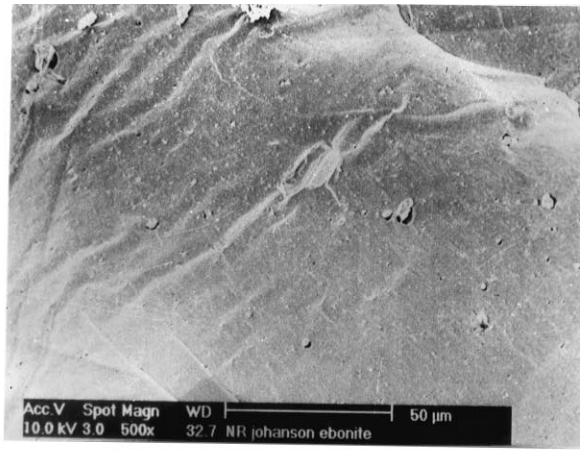

NR

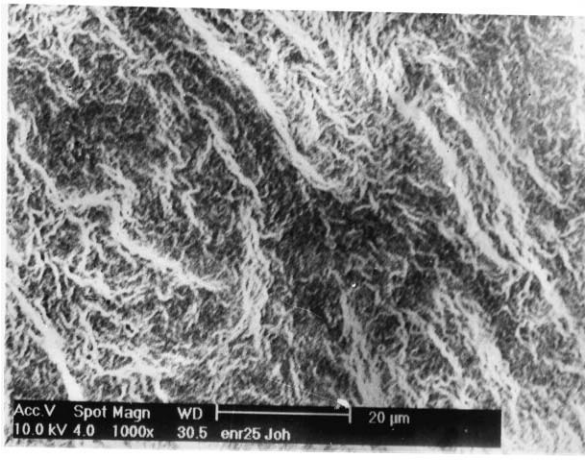

ENR-25

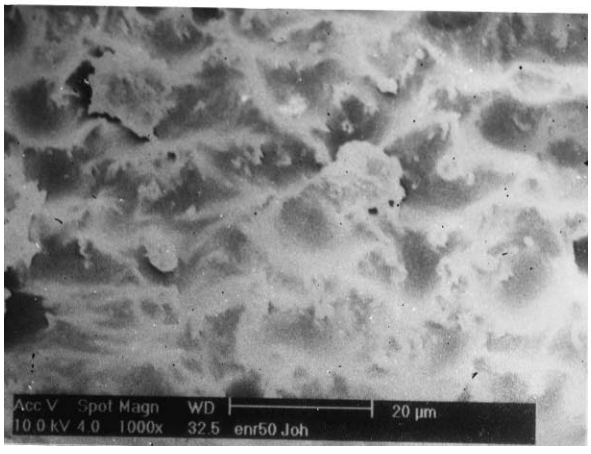

Fig. 8. Surface morphology of NR, ENR-25 and ENR-50.

molecules may be trapped in the highly crosslinked gel phase resulting in a mass gain. The Q_∞ values for resorption and redesorption cycles are close to each other indicating no further mass loss or mass gain. The equilibrium uptake for resorption run in the case of NR increases. This may be due to the increase in free volume of NR matrix due to leaching

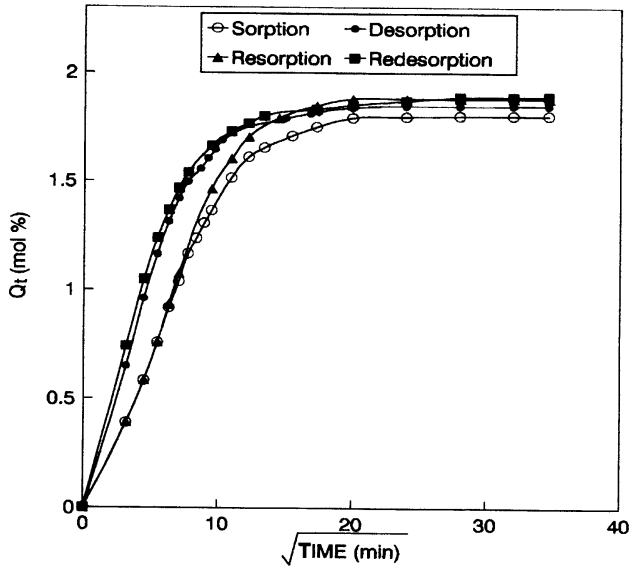

Fig. 9. Sorption (S)–desorption (D)–resorption (RS)–redesorption (RD) curves for NR in hexane at 27°C.

out of unreacted compounding ingredients during the sorption–desorption cycle.

3.4. Kinetics of diffusion

When barrier applications of polymers are to be considered in separation problems, their swelling kinetics is important. As long as the polymer thickness does not increase substantially, the first-order kinetics seems to be applicable to the diffusion-controlled swelling [29,30]. Thus attempts are made to calculate the first-order kinetic rate constants k_1 for the membrane–solvent systems [31]

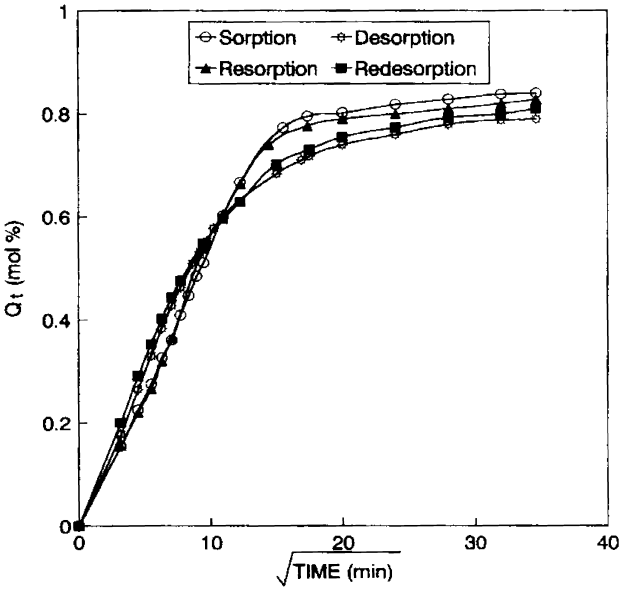

Fig. 10. Sorption (S)–desorption (D)–resorption (RS)–redesorption (RD) curves for ENR-25 in hexane at 27°C.

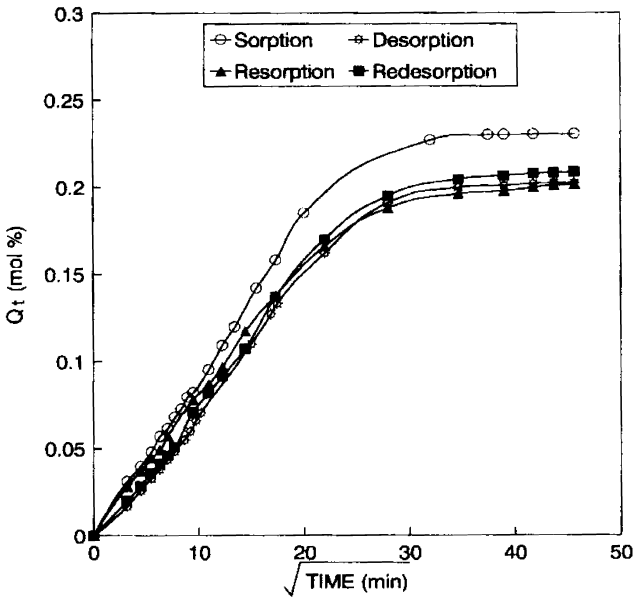

Fig. 11. Sorption (S)–desorption (D)–resorption (RS)–redesorption (RD) curves for ENR-50 in hexane at 27°C.

using the first-order rate equation

$$\frac{dc}{dt} = k_1(C_\infty - C_t) \tag{2}$$

where k_1 is the first-order rate constant, C_∞ and C_t are the concentrations at equilibrium and at time t.

Integration of Eq. (2) gives

$$kt = 2.303 \log[C_\infty/C_\infty - C_t] \tag{3}$$

The values of rate constants obtained by the least square analysis of the plot of log $(C_\infty - C_t)$ against time are given in Table 4. The correlation coefficient in the determination of the first-order kinetic rate constants was found to be 0.99. It is observed that the rate constant values decrease as epoxidation level increases, suggesting rate of diffusion to be smaller as the chain flexibility decreases. But as the temperature increases, k values increase suggesting increased chain flexibility with a corresponding increase in the rate constant values.

Table 4
Rate constant values $k \times 10^2$ (min^{-1})

Solvent	Temperature (°C)	NR	ENR-25	ENR-50
Pentane	27	2.41	1.82	0.52
Hexane	27	1.3	1.03	0.33
	40	1.7	1.20	0.45
	50	1.81	1.31	0.48
	60	1.94	1.50	0.58
Heptane	27	1.37	0.69	0.35
	40	1.27	0.92	0.41
	50	1.38	0.79	0.43
	60	1.54	1.1	0.542
Octane	27	0.98	0.54	0.28
	40	1.1	0.61	0.31
	50	1.18	0.68	0.37
	60	1.21	0.74	0.42

3.5. Diffusivity

For a Fickian transport, the sorption curves are generally independent of material thickness. If there is a negligible concentration dependence of diffusivity over the concentration interval studied, a value of mutual diffusion coefficient D can be calculated using the equation [32]

$$\frac{Q_t}{Q_\infty} = 1 - \sum_{x=0}^{\infty} \frac{8}{(2x+1)^2\pi^2} e^{-(2x+1)^2\pi^2(Dt/h^2)} \tag{4}$$

where t is the time and h is the initial thickness of the polymer sheet. Although this equation can be solved readily, it is instructive to examine the short-time limiting expression as well

$$\frac{Q_t}{Q_\infty} = [4/\pi^{1/2}][Dt/h^2]^{1/2} \tag{5}$$

From a plot of Q_t vs. $t^{1/2}$, a single master curve is obtained which is initially linear. Thus, D can be calculated from a rearrangement of Eq. (5) as

$$D = \pi[h\theta/4Q_\infty]^2 \tag{6}$$

where θ is the slope of the graph of Q_t vs. $t^{1/2}$.

The values of D given in Table 5 shows that, the diffusion constant decreases with increasing level of epoxidation and increases with increase of temperature. This observation is supported by the values of rate constant given in Table 4. However, Fig. 12 shows that the diffusion coefficient values decrease with increase in molecular weight of solvents even though the Q_∞ values increase with molecular weight except for octane. This supports the concept of inverse dependence of diffusion coefficient on the molecular weight of solvents [33].

Table 5
Diffusion coefficient $D \times 10^7$ ($cm^2\ s^{-1}$)

Solvent	Temperature (°C)	NR	ENR-25	ENR-50
Pentane	27	15.89	9.5	1.80
Hexane	27	8.9	5.4	1.1
	40	11.81	7.1	1.78
	50	12.65	7.4	1.98
	60	13.63	7.1	2.17
Heptane	27	8.10	3.49	1.06
	40	9	4.84	1.39
	50	10.47	4.64	1.75
	60	12.01	6.34	2.05
Octane	27	7.4	3.1	0.98
	40	7.7	3.8	1.14
	50	8.4	4.2	1.28
	60	8.8	5.1	1.37

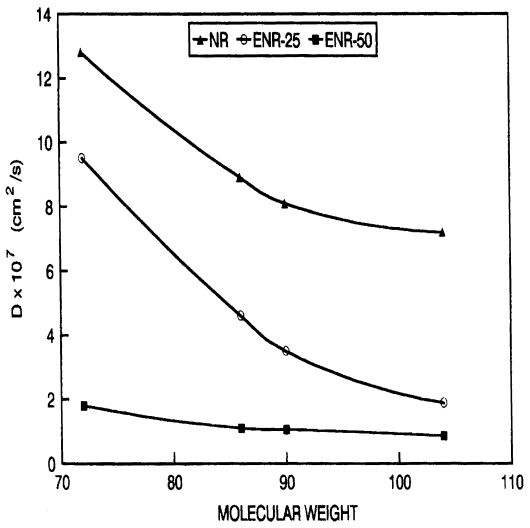

Fig. 12. Dependence of diffusion coefficient on the molecular weight of solvents.

3.6. Sorption and permeation coefficients

In order to obtain a better understanding on the strength of interactions between polymer and solvents as the epoxidation level increases, the sorption coefficient, which is a thermodynamic parameter has been calculated using the relation

$$S = \frac{M_\infty}{M_0} \tag{7}$$

Further permeability coefficients of solvent molecules have been calculated as it depends both on diffusivity and sorptivity using the relation [34,35].

$$P = DS \tag{8}$$

where D is diffusion coefficient and S denotes sorption coefficients.

Table 6 shows the values of S and P. NR has the maximum value for sorption constant and ENR-50 the minimum. But with increase in temperature sorption coefficients for NR decreases while for ENR-25 and ENR-50, value of S increases. This may be due to the negative heat of sorption for NR. Permeation coefficient decreases with level of epoxidation but it increases with temperature in all the three cases. But P and S values increase with increase in penetrant size up to heptane but decrease for octane. This is due to the increased polymer–penetrant interaction in the former case. This is reflected in the interaction parameter values reported later.

3.7. Activation parameters

Activation energy for diffusion E_D and that for permeation E_P has been calculated using the Arrhenius equation,

$$\log X = \log X_0 - (E_x/2.303RT) \tag{9}$$

where X represents either D or P, X_0 is a constant representing either D_0 or P_0. E_x is either E_D or E_P. Arrhenius plot of $\log D$ vs. $1/T$ for calculating the activation parameters is given in Fig. 13. Values of E_D and E_P are presented in Table 7. The E_D and E_P values vary from 0.001 to 0.003. It is seen that with increase in solvent resistance, i.e. as the epoxidation level increases, both E_P and E_D values increase. Also with increase in size of the penetrant molecules, activation energy values increase.

3.8. Enthalpy and entropy of sorption

Thermodynamic sorption constant K_s defined as [36]

$$K_s = \frac{\text{No. of moles of solvent sorbed at equilibrium}}{\text{Mass of the polymer sample}} \tag{10}$$

Table 6
Values of S and P

Solvent	Temperature (°C)	S			$P \times 10^6$ (cm^2 s^{-1})		
		NR	ENR-25	ENR-50	NR	ENR-25	ENR-50
Pentane	27	1.116	0.4841	0.176	1.77	0.46	0.03
Hexane	27	1.73	0.705	0.201	1.5	0.38	0.023
	40	1.50	0.95	0.236	1.65	0.38	0.042
	50	1.55	0.987	0.279	1.8	0.522	0.055
	60	1.59	1.12	0.365	2.01	0.577	0.057
Heptane	27	2.13	1.069	0.315	1.73	0.373	0.035
	40	2.06	1.148	0.338	1.86	0.540	0.047
	50	1.99	1.197	0.398	2.09	0.555	0.069
	60	2.07	1.234	0.454	2.49	0.782	0.093
Octane	27	1.02	0.431	0.124	0.7548	0.133	0.012
	40	1.12	0.452	0.126	0.8624	0.171	0.014
	50	1.18	0.471	0.131	0.9912	0.197	0.016
	60	1.24	0.521	0.133	1.091	0.265	0.018

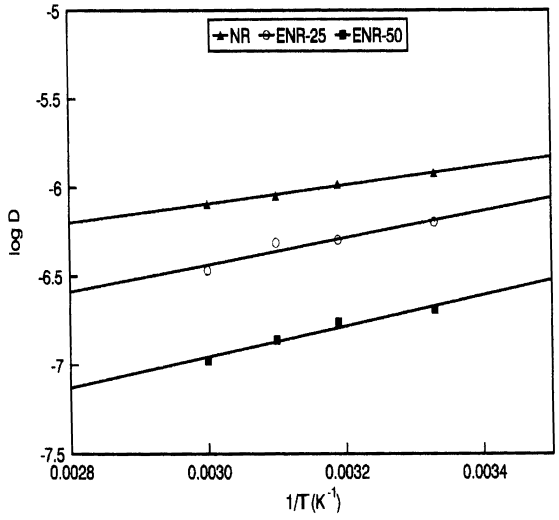

Fig. 13. Arrhenius plot of log D vs. $1/T$.

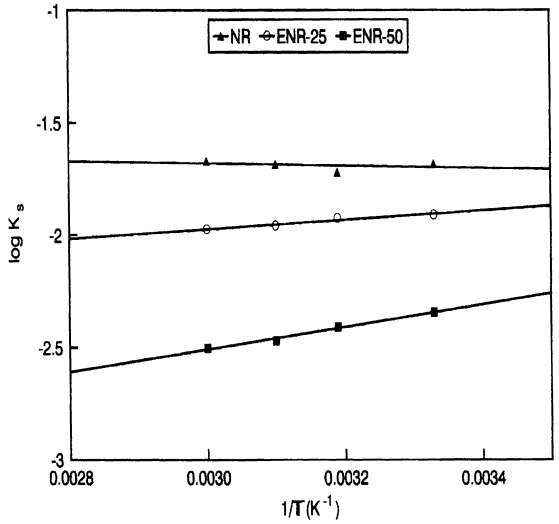

Fig. 14. Van't Hoff plot of log ks vs. $1/T$.

has been used to calculate the enthalpy ΔH_s and entropy ΔS of sorption using the Van't Hoffs relation

$$\log K_s = \Delta S/2.303\mathrm{R} - \Delta H_s/2.303RT \quad (11)$$

A typical Van't Hoffs plot is shown in Fig. 14 and the values of ΔH_s and ΔS are given in Table 8. The uncertainty in the values range from ± 0.001 to ± 0.004. ΔS values decrease with epoxidation suggesting decreased disorder of solvent molecules. Enthalpy of sorption is negative for NR and positive for ENR-25 and ENR-50. The enthalpy of sorption is a composite parameter involving the contribution from: (i) Henry's law needed for the formation of a site and the dissolution of the species into that site-the formation of the site involves an endothermic contribution; and (ii) Langmuir's (hole filling) type sorption mechanism, in which case the site already exists in the polymer matrix and sorption by hole filling gives exothermic heats of sorption. The negative ΔH_s values for NR suggests a Langmuir type sorption in NR and the positive values of ENR suggests a Henry's type sorption in ENR.

3.9. Interaction parameter

In order to follow the effect of polymer–solvent interaction, the values of interaction parameter χ have been calculated using the equation, [37]

$$\chi = \beta + V_s/\mathrm{R}T(\delta p - \delta s)^2 \quad (12)$$

Table 7
Values of activation parameter, E_P and E_D

Solvent	E_P (kJ mol^{-1})			E_D (kJ mol^{-1})		
	NR	ENR-25	ENR-50	NR	ENR-25	ENR-50
Hexane	3.257	7.052	11.87	3.89	6.02	7.26
Heptane	4.12	7.64	11.91	4.38	6.48	7.37
Octane	4.53	7.83	12.04	4.78	6.78	7.52

Table 8
Values of ΔH and ΔS

Solvent	ΔH (kJ mol^{-1})			$-\Delta S$ (J mol^{-1} K^{-1})		
	NR	ENR-25	ENR-50	NR	ENR-25	ENR-50
Hexane	−12.71	3.96	7.58	10.90	25.01	33.9
Heptane	−13.46	6.46	9.34	17.08	24.65	36.21
Octane	−15.82	7.28	9.84	21.08	28.84	47.24

where V_s is the molar volume of the solvent, δp and δs are the solubility parameters of the polymer and solvent respectively. R is the universal gas constant and T is the temperature.

The χ values are tabulated in Table 9. The lowest value is obtained for NR suggesting higher interaction of NR with the penetrants. Further the interaction of heptane with polymer is greater compared to other solvents. This is in agreement with the solvent uptake.

3.10. Determination of the network structure

The investigation of swelling equilibrium can help to elucidate the structure of the polymer network. The Flory and Rehner [38] relations were developed for a network deforming affinely, i.e. the components of each chain vector transform linearly with macroscopic deformation and the junction points are assumed to be embedded in the network without fluctuations. The molecular weight between

Table 9
Values of interaction parameter χ

Solvent	NR	ENR-25	ENR-50
Hexane	0.414	0.781	1.21
Heptane	0.363	0.535	1.06
Octane	0.435	0.812	1.34

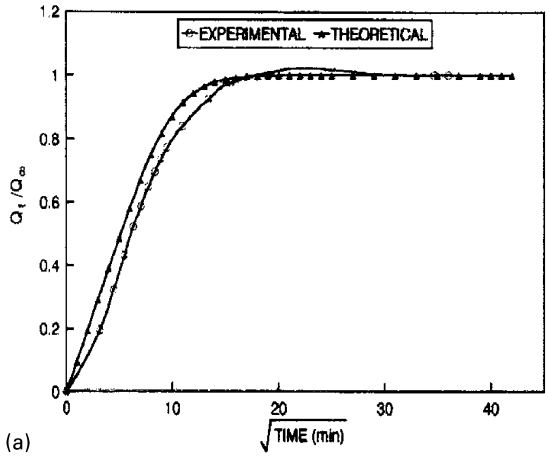

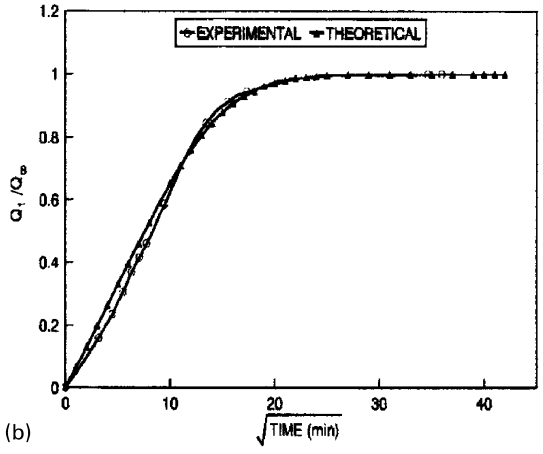

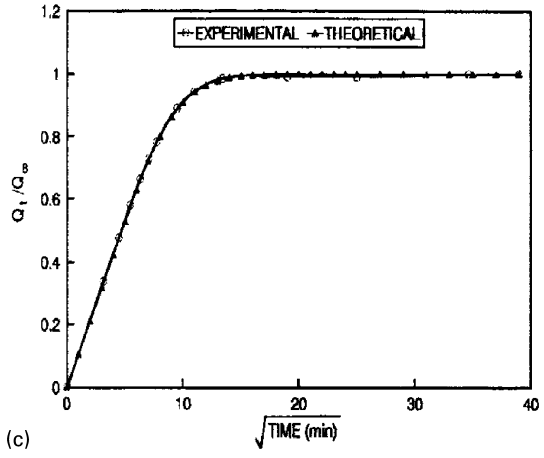

Fig. 15. Theoretical comparison in hexane at 27°C for: (a) NR; (b) ENR-25; and (c) ENR-50.

Table 10
Comparison of swelling equilibrium properties in hexane

M_c values	NR	ENR-25	ENR-50
M_c(chem)	4897	3612	909
M_c(aff)	4540	3310	833
M_c(ph)	1513	1103	277

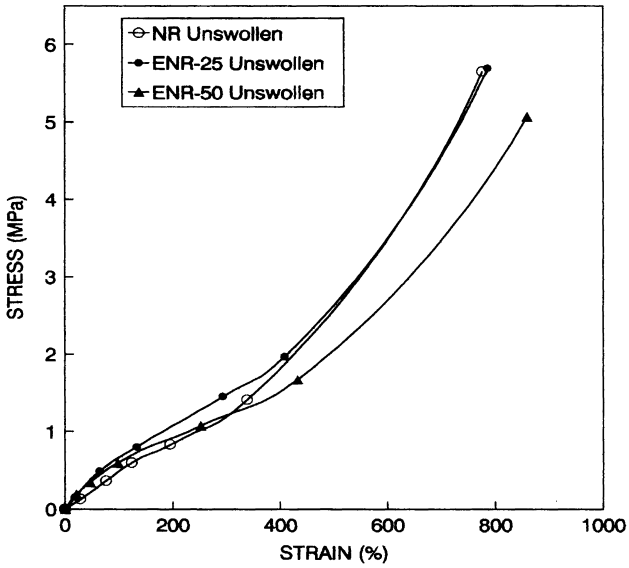

Fig. 16. Stress–strain curves of NR, ENR-25 and ENR-50 in unswollen state.

crosslinks (M_c) for the affine limit of the model [M_c(affi)] can be calculated by the formula, [39]

$$M_c(\text{affi}) = \frac{\rho V_s \nu_{2c}^{2/3} \nu_{2m}^{1/3}\left(1 - \frac{\mu}{\nu}\nu_{2m}^{1/3}\right)}{-(\ln(1-\nu_{2m}) + \nu_{2m} + \chi\nu_{2m}^2)} \quad (13)$$

where V_s is the molar volume of the solvent, μ and ν are called the number of effective chains and junctions; ν_{2m}, the polymer volume fraction at swelling equilibrium; ν_{2c}, the polymer volume fraction during crosslinking; and ρ, the polymer density. James and Guth [40] proposed the phantom network model, where the chain may move freely through one another. According to the theory, the molecular weight between crosslinks for the phantom limit of the model [M_c(ph)] was calculated by [39,41]

$$M_c(\text{ph}) = \frac{\left(1 - \frac{2}{\phi}\right)\rho V_s \nu_{2c}^{2/3} \nu_{2m}^{1/3}}{-(\ln(1-\nu_{2m}) + \nu_{2m} + \chi\nu_{2m}^2)} \quad (14)$$

where ϕ is the junction functionality.

M_c(aff) and M_c(ph) were compared with M_c(chem) and the values are given in Table 10. It is seen that M_c(chem) values are close to M_c(aff). This suggests that in the highly swollen state, NR, ENR-25 and ENR-50, the network deform affinely.

3.11. Comparison with theory

The experimental diffusion results were compared with theoretical predictions using the relation [42]

$$\frac{Q_t}{Q_\infty} = 1 - \frac{8}{\pi^2}\sum_{n=0}^{n=\infty}\frac{1}{(2n+1)^2}\exp\left[-D(2n+1)^2\pi^2 t/h^2\right] \quad (15)$$

where Q_t and Q_∞ are the mass of mole percent solvent uptake at time t, and at equilibrium and h is the initial

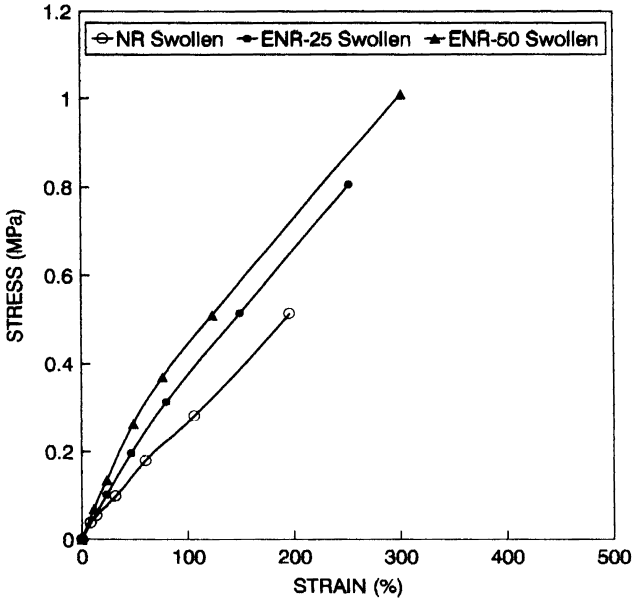

Fig. 17. Stress–strain curves of NR, ENR-25 and ENR-50 in swollen state.

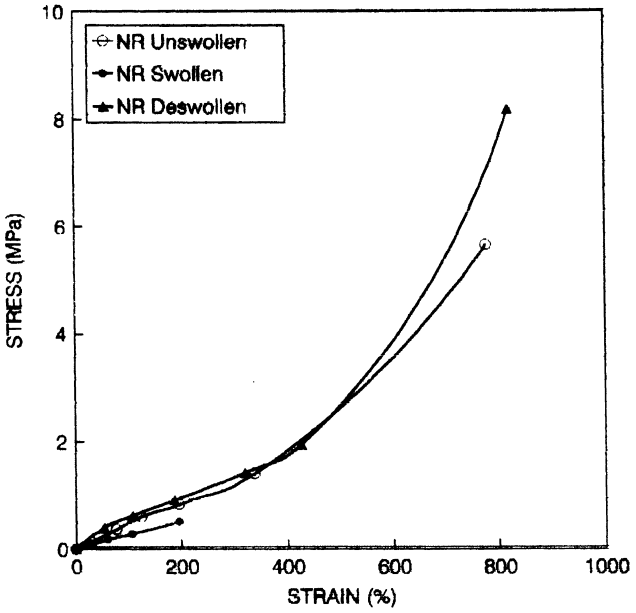

Fig. 19. Stress–strain curves of unswollen, swollen and deswollen NR samples.

sample thickness. The given equation represents a Fickian mode of diffusion. The experimentally determined values of diffusion coefficient (D) for NR, ENR-25 and ENR-50 were substituted in the equation and the curves obtained are given in Fig. 15a–c. From the figures it is clear that mechanism of diffusion is anomalous for NR and ENR-25, whereas it is close to Fickian for ENR-50. Thus it is seen that the mechanism approaches the Fickian mode with an increase in the epoxidation level.

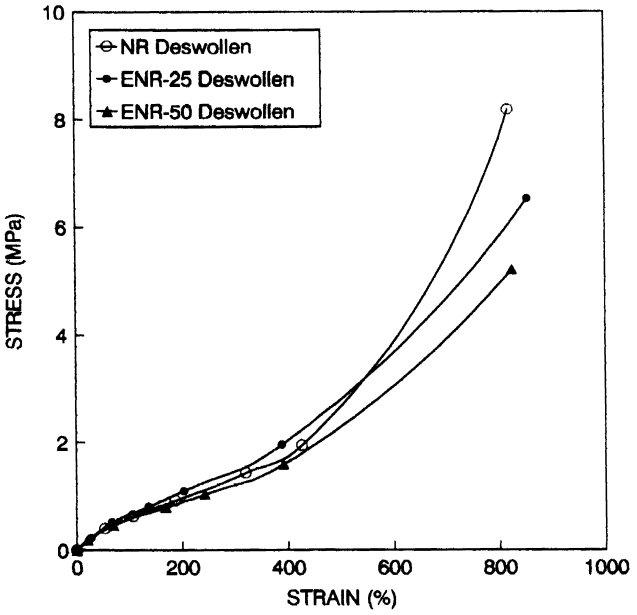

Fig. 18. Stress–strain curves of NR, ENR-25 and ENR-50 in deswollen state.

4. Mechanical properties

4.1. Stress–strain behaviour under tension

In the unswollen state (Fig. 16) all the three samples, NR, ENR-25 and ENR-50 exhibit typical elastomeric curves. The increase in stress at higher strain is due to the strain crystallising nature of NR. The strain crystallising nature decreases in the order NR > ENR-25 > ENR-50. This is because epoxidation affects the stereo regular nature of NR [43]. The stress is maximum for NR, which decreases slightly in going to ENR-50. This proves that even after 50% epoxidation NR retains its strain crystallising nature [22]. The swollen samples (Fig. 17) does not exhibit the typical elastomeric behaviour. This may be due to the loss of strain crystallising nature. As the per cent of epoxidation increases, the resistance to swelling also increases which is reflected in the higher stress values of ENR-25 and ENR-50.

Fig. 18 represents the stress–strain curves of deswollen samples. The observed trend is exactly same as that of unswollen state. Further on comparing the stress–strain curves of swollen, deswollen and unswollen samples of NR, ENR-25 and ENR-50 (Figs. 19–21) it can be seen that in all the cases the deswollen samples exhibit maximum stress value. This is due to the enhanced interchain interaction in deswollen samples. The leaching out of unreacted compounding ingredients during swelling makes the interchain interaction stronger than the unswollen state. Also, Fig. 18 shows that the maximum stress value of deswollen NR is much higher than deswollen ENR-25 and ENR-50. This may be due to the increased leaching out of unreacted compounding ingredients from NR due to its greater chain

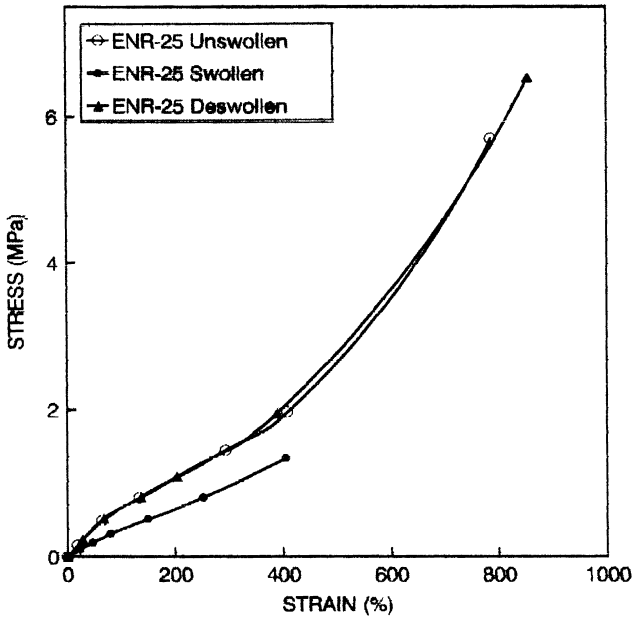

Fig. 20. Stress–strain curves of unswollen, swollen and deswollen ENR-25 samples.

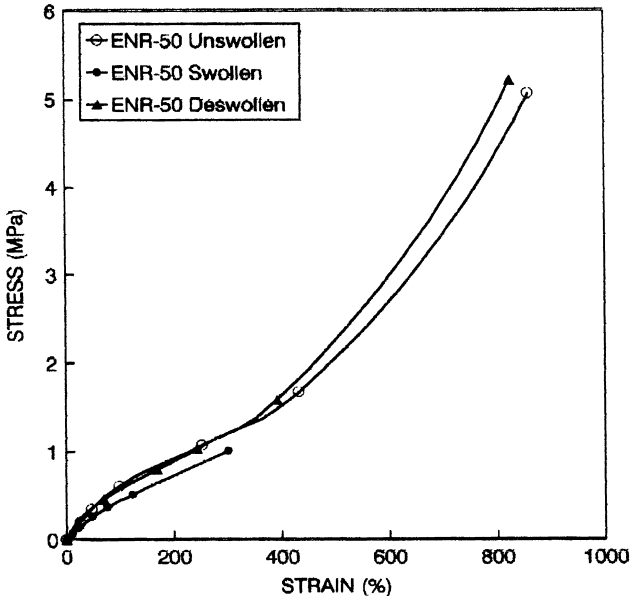

Fig. 21. Stress–strain curves of unswollen, swollen and deswollen ENR-50 samples.

flexibility. The T_g values given earlier indicates the increased chain flexibility.

The tensile behaviour of unswollen NR, ENR-25 and ENR-50 are presented in Table 11. As expected the tensile strength is maximum for NR and minimum for ENR-50. This is due to the reduction in strain crystallising nature of NR with epoxidation. The observed variation in tensile strength can be correlated with the crosslink density values (Table 11) calculated using the equation [44]

$$n' = \frac{F}{2A_0\rho_p RT(\alpha - 1/\alpha^2)} \tag{16}$$

where F is the force required to stretch a specimen to an extension ratio α, A_0, the cross-sectional area of the sample, R, the universal gas constant and T, the absolute temperature.

It is observed that elongation at break decreases from NR to ENR-50. The highest value in NR is due to strain crystallisation. These observations suggest that the EB variation depend on the stereo regularity of the NR matrix.

The Young's modulus of a material reflects the stress at low strain while secant modulus values (M_{100}, M_{200}, M_{300}) reflect the stress at higher strains. As can be seen from Table 9, Young's modulus values increase from NR to ENR-50. This means that at low strain level, stretching of NR is easy compared to ENR-25 and ENR-50. This is attributed to the coiled structure of NR that leads to a soft (low modulus) material [43]. The behaviour at higher strain is just reverse of earlier case. At higher strains, since the strain crystallising nature of NR is prominent compared to ENR-25 and ENR-50 the modulus values for NR is greater than ENR-25 and ENR-50.

In the swollen state, all the mechanical properties are found to be inferior compared to unswollen state (Table 11). Crosslink density values of the swollen state are much lower compared to the unswollen state. It has been reported by Mullins [45] that the density of crosslinks

Table 11
Mechanical data

Sample	System	Tensile strength (MPa)	E.B. (%)	Crosslink density ($\nu \times 10^5$) (gmol cm^{-3})	Young's modulus (MPa)	Secant modulus (MPa)		
						M_{100}	M_{200}	M_{300}
Unswollen	NR	9.03	930	6.08	2.15	0.8125	1	1.375
	ENR-25	6.49	921	4.23	2.30	0.625	1	1.25
	ENR-50	5.81	917	3.58	2.70	0.593	0.937	1.125
Swollen	NR	0.5169	237	5.60	0.78	0.29	0.48	–
	ENR-25	1.26	400	3.30	1.4	0.40	0.73	1.04
	ENR-50	1.11	336	3.43	1.5	0.42	0.73	1.01
Deswollen	NR	11.3	910	7.7	2.9	0.69	1.26	1.81
	ENR-25	6.56	863	4.55	3.5	0.68	1.07	1.52
	ENR-50	6.02	834	4.06	3.5	0.576	0.87	1.28

determined by physical methods (swelling or stress–strain behaviour) is always higher than the actual density of chemically inserted crosslinks. However, in the swollen state the plasticisation of the polymer matrix by the solvent affects the physical interactions between the polymer chains, the effect being greater for NR. This results in the decreased values of crosslink density in the swollen state. However, the extensive plasticisation of NR matrix by the solvent results in its lower crosslink density values compared to ENR-25 and ENR-50. Further, in the swollen state, the tensile strength increases from NR to ENR-50 that is in agreement with crosslink density values. The Young's and secant moduli values are indicative of the increased swelling resistance in ENR samples.

For the deswollen samples, the observed trend in mechanical properties is similar to the unswollen case (Table 11). Nevertheless there is an overall enhancement in the magnitude of the values. This is attributed to the increased interchain interaction as a result of leaching out of the unreacted compounding ingredients from the matrix.

5. Conclusion

Effect of epoxidation on molecular transport of aliphatic hydrocarbons in NR has been studied. The maximum solvent uptake values decrease in the order NR > ENR-25 > ENR-50, reflecting the improved solvent resistance with epoxidation. Rate of diffusion and diffusion coefficient decrease as we move from NR to ENR-50 due to decreased chain flexibility. Permeation and sorption coefficients show similar trend. But sorption coefficients decrease with temperature for NR due to negative heat of sorption. Permeation and sorption coefficients increase with penetrant size from pentane to heptane but decreases for octane, reflecting the increased polymer–solvent interaction for pentane, hexane and heptane. The values of E_P and E_D reflect the solvent resistance of ENR. Interaction parameter values confirm the observation of polymer–solvent interaction. Comparison with theory establishes that the mechanism of diffusion is anomalous for NR and ENR-25 whereas the mechanism approaches Fickian for ENR-50. Investigation of the network structure in the swollen state show that the network deforms affinely in the swollen state. The improved mechanical properties of NR over ENR result from its strain crystallising nature. Swollen samples show weaker mechanical properties due to loss of strain crystallisation. Improved polymer–polymer interaction in deswollen samples leads to better mechanical properties compared to unswollen samples.

Acknowledgements

One of the authors (T. Johnson) is thankful to University Grants Commission for the award of Junior Research Fellowship.

References

[1] Powell PC. Engineering with Polymers. New York: Chapman and Hall, 1983.
[2] Aminabhavi TM, Cassidy PE, Kukacka LE. J Macromol Sci Rev Macromol Chem Phys C 1982/1983;22:1.
[3] Aminabhavi, TM, Cassidy PE, Biradar NS. J Macromol Sci Rev Macromol Chem Phys 1987/1988;27(3 and 47):459.
[4] Rao RV, Yassen M. Pigment Resin Technol 1978;7:4.
[5] Ruggeri RT, Beck TR. Org Coat Plast Chem 1980;43:583.
[6] Koszinowski J. J Appl Polym Sci 1986;32:4765.
[7] Berns AR, Hopfenberg HB. J Membr Sci 1982;10:283.
[8] Hwang ST, Choi CK, Kammermeyer K. Sep Sci 1974;9:461.
[9] Robinson JR. Sustained and Controlled Release of Drug Delivery Systems. New York: Dekker, 1978.
[10] Hung GWC, Autian J. J Pharm Sci 1972;61:1094.
[11] Sefton MV, Mann JJ. Appl Polym Sci 1984;25:829.
[12] Schneider NS, Illinger JL, Cleaves MA. Polym Engng Sci 1986;26:1547.
[13] Chiang KT, Sefton MV. J Polym Sci Polym Phys 1977;15:1927.
[14] Rennar N, Oppermann W. Colloid and Polym Sci 1992;270:527.
[15] Jain SR, Sekkar V, Krishnamurthy VN. J Appl Polym Sci 1993;45:1515.
[16] Unnikrishnan G, Thomas S. Polymer 1994;35:5504.
[17] Mathew AP, Packirisamy S, Kumaran MG, Thomas S. Polymer 1995;36:4935.
[18] George SC, Ninan KN, Thomas S. Polymer 1996;37(26):5839.
[19] Mathai AE, Thomas S. Macromol Sci Phys B 1996;35(2):229.
[20] Perera MCS, Elix JA, Bradbury JH. J Appl Polym Sci 1988;36:105.
[21] Perera MCS. J Appl Polym Sci 1987;34:2591.
[22] Davies CKL, Wolfe SV, Gelling IR, Thomas AG. Polymer 1983;24:107.
[23] Fujimoto K, Nishi T, Okamoto T. Int Polym Sci Technol 1981;8(8):T/30.
[24] Baker CSL, Gelling IR, Newell R. Rubber Chem Technol 1994;58:67.
[25] Uragami T, Morikawa T, Okuno H. Polymer 1989;30:1117.
[26] Okuno H, Nishimoto H, Miyata T, Uragami T. Makromol Chem 1993;194:927.
[27] Davey JE, Loadman MJR. Br Polym J 1984;16:134.
[28] Burfield DR, Lim KK, Law KS, Ng S. Polymer 1984;25(7):995.
[29] Ofner CM, Schott H. J Pharm Sci 1986;75:790.
[30] Schott H. J Macromol Sci Phys B 1992;31:1.
[31] Aminabhavi TM, Harogoppad SB. J Chem Educ 1994;68:343.
[32] Crank JS. The Mathematics of Diffusion. 2nd ed. Oxford: Clarendon Press, 1975.
[33] Unnikrishnan G, Thomas S. J Polym Sci B Polym Phys Ed 1997;35:725.
[34] Harogoppad SB, Aminabhavi TM. Macromolecules 1991;24:2595.
[35] Aminabhavi TM, Harogoppad SB. J Chem Educ 1994;68:343.
[36] Hung GWC. J Microchem 1974;19:130.
[37] Aithal US, Aminabhavi TM, Cassidy PE. In: Koros WJ, editor. Barrier Polymers and Structures, 197th National ACS Meeting, Dallas, TX. American Society Symposium SeriesWashington, DC: American Chemical Society, 1989 (351pp).
[38] Flory PJ. Principles of Polymer Chemistry. Ithaca: Cornell University Press, 1953.
[39] Treloar LRG. The Physics of Rubber Elasticity. Oxford: Clarendon Press, 1975.
[40] James HM, Guth E. J Chem Phys 1947;15:669.
[41] Mark JE, Erman B. Rubber Like Elasticity, a Molecular Primer. New York: Wiley, 1988.
[42] Aithal US, Aminabhavi TM. J Chem Educ 1990;67:82.
[43] Gelling IR. Rubber Chem Technol 1985;58:86.
[44] Mark HF, Bikales NM, Overberge CG, Menges G. Encyclopaedia of Polymer Science and Engineering, vol. 4. New York: Wiley, 1986 (356pp.).
[45] Mullins L. J. Appl Polym Sci 1959;2:1.